

Study on diffusion behavior of water in epoxy resins cured by active ester

Mojun Liu, Peiyi Wu,* Yifu Ding and Shanjun Li*

Department of Macromolecular Science and The Key Laboratory of Molecular Engineering of Polymers, Ministry of Education, Fudan University, Shanghai 200433, China.
E-mail: sjli@fudan.edu.cn

Received 9th September 2002, Accepted 11th March 2003

First published as an Advance Article on the web 27th March 2003

Phenol novolac resin and a series of esterified phenol novolac resins with side groups of acetate, butyrate and phenylacetate are used as curing agents for O-Cresol novolac epoxy resin. The cured resins are named as EP, EPA, EPB and EPP respectively. The water diffusion behavior of epoxy networks is studied by ATR-FTIR spectroscopy and gravimetric method. The obtained results show that the diffusion type of EPA and EPP are quite approximate to Fickian diffusion, while EPB displays a typical Case II characteristic and EP follows anomalous diffusion. The diffusion coefficient of EP is much lower than EPA and EPP. In 2D-IR spectra the splitting of water OH vibration band in the range of $2800\text{--}3700\text{cm}^{-1}$ and $1500\text{--}1800\text{cm}^{-1}$ shows the existence of two different states of water as free and bound water. Water molecules first bind with specific hydrophilic groups as bound water and then diffuse into free volume (microvoids) or molecularly disperse with less hydrogen bonding (bulk dissolve) as free water. Evidence is also found for the strength order of hydrogen bonding interactions between water molecules and epoxy networks as $\text{EP} > \text{EPA} > \text{EPB} > \text{EPP}$.

1. Introduction

There has been a long standing interest in water sorption in epoxy networks^{1–6} because water sorption would bring about a deterioration in excellent properties of epoxy resins. Water sorption is related to the availability of molecular-sized free volume holes in the epoxy networks and epoxy–water interactions. The availability of holes depends on the polymer structure, morphology and crosslink density. Furthermore water–epoxy interaction depends on the presence of hydrogen bonding sites in the polymer networks. The nature of epoxy–water molecular interactions has been studied by various techniques. Woo and Piggott⁷ suggest clustering of water molecules in epoxy resins. Apicella *et al.*⁸ proposes three sorption models in glassy epoxy: bulk dissolution of water in glassy epoxy networks; moisture sorption onto the surface of excess free volume; hydrogen bonding between water and epoxy hydrophilic groups. As a results, Adamson⁹ concludes that water molecules first occupy free volume holes then become bound to networks hydrophilic groups which causing swelling, finally, enter the densely crosslinked regions. Moy, Karasz¹⁰ and Pethrick¹¹ report the existence the free/bound water types in epoxy resins. However, substantial disagreement still persisted among these models due to their different experimental methods.

Recently, following the pioneering work of Fieldsen and Barbari,^{12,13} the ATR-FTIR technique has been quickly developed to provide *in situ* measurements of both ingress and removal of water from polymer systems.^{14–16} The application of this technique relies on the spectroscopic observation of penetrate localized within a short distance ($0.5\text{--}5\mu\text{m}$) from the interface between polymer sample and the IRE crystal. It provides not only reliable mass-time sorption curves but also rich information of the polymer–water molecular interactions, which in many systems, are the key factor that control the sorption behavior.

The generalized two-dimensional (2D) IR spectroscopy proposed by Noda^{17–19} has rapidly received great attention in

recent years. It emphasizes spectral features not readily observable in conventional one-dimensional (1D) spectra and also probes the specific order of certain events taking place with the development of a controlling physical variable. It assists the identification of various inter- and intramolecular interactions through the selective correlation of bands.²⁰

Aim of the present contribution is to describe in detail the water diffusion behavior of a series of epoxy networks with similar backbone but different side groups by gravimetric method and ATR-FTIR spectroscopy. In particular, attention has been focused onto the diffusion kinetics and the changes of different epoxy–water interactions during the diffusion process.

2. Experimental

2.1. Materials

O-cresol (2-methyl phenol) novolac epoxy resin (YDCN-702p from Tohto Kasei, Japan, epoxy equivalent: $200\text{--}230\text{ g eq}^{-1}$) and Novolac (H-1, from Sumitomo, Japan, hydroxyl equivalent: 107 g eq^{-1}) were used in this work. The esterified curing agents were synthesized from novolac (NOV), acetic anhydride, butyric anhydride and phenylacetyl chloride according to the procedure reported previously.^{21,22} 2-methylimidazole (2MI, from Wuhan Pharmaceutical Co., China) was used as curing accelerator.

2.2. Sample preparation

The fresh mixture of epoxy resins, the curing agents and 0.5% of 2-MI was dissolved in AR acetone. Then the solution was casted onto a $75\text{ mm} \times 25\text{ mm} \times 1\text{ mm}$ microscope slide. After being left in the air at room temperature on a metal plate for 1 d, the resins were cured in a vacuum oven at 45°C (15 min^{-1}), 80°C (15 min^{-1}), 120°C (3 h^{-1}), 150°C (2 h^{-1}), 180°C (2 h^{-1}), and finally cooled slowly down to room temperature. Then the films were peeled off for ATR experiments. The curing procedures of the samples used for gravimetric measurements were

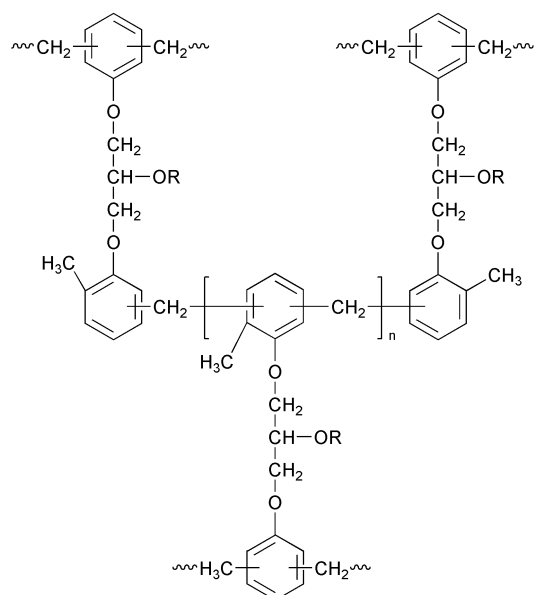


Fig. 1 Chemical structures of cured epoxy resins EP, EPA, EPB and EPP: for EP, R = H; for EPA, R = CH₃CO; for EPB, R = CH₃CH₂CH₂CO; for EPP, R = Ph-CH₂CO.

same as above, while before curing the solution was poured into a 50 mm × 20 mm × 20 mm aluminium mold. The thickness of the sample films was measured by a Coatest-1000 (UK) nonferrous digital coating thickness gauge. The chemical structures of the cured resins EP, EPA, EPB and EPP are shown in Fig. 1.

2.3. Gravimetric measurements

The sample sheets (10 mm × 10 mm × 1 mm) were washed with distilled water and then dried under vacuum oven at 85 °C for a week. Water sorption in the resins as the function of immersion time was monitored by gravimetric method. The samples were periodically removed from the water of 20 °C, wiped down and quickly weighed on a Tg332A microbalance (accuracy: ±0.01 mg). The water sorption (uptake at time t , M_t) of the sample is

$$M_t = 100(W_t - W_0)/W_0$$

W_t is the weight of the wet specimen at time t and W_0 is the weight of the dry specimen.

2.4. Time-resolved ATR-FTIR measurements

Time-resolved ATR-FTIR measurements were performed at 24 °C using a Nicolet Nexus Smart ARK FTIR spectrometer equipped with a DTGS-KBr detector and a ZnSe IRE crystal. The spectra were measured at 4 cm⁻¹ resolution and the wavenumber range was 650–4000 cm⁻¹. The film-covered IRE crystal with a filter paper above the sample film was mounted in an ATR cell and the spectra of the dry film was collected as background spectra, then without moving the sample, distilled water was injected into the filter paper while starting the data acquisition by a macro program. A typical sorption loop lasts about 15 min and the acquisition time interval was 27 s. The time-resolved ATR-FTIR spectra of sorbed water in two wavenumber ranges were obtained from subtraction spectra of the background and the wet sample films (in Fig. 2).

2.5. Two-dimensional correlation analysis

Several spectra at equal time intervals in a certain wavenumber range were selected for 2D correlation analysis using the software “2D Pocha” written by Daisuke Adachi (Kwansei

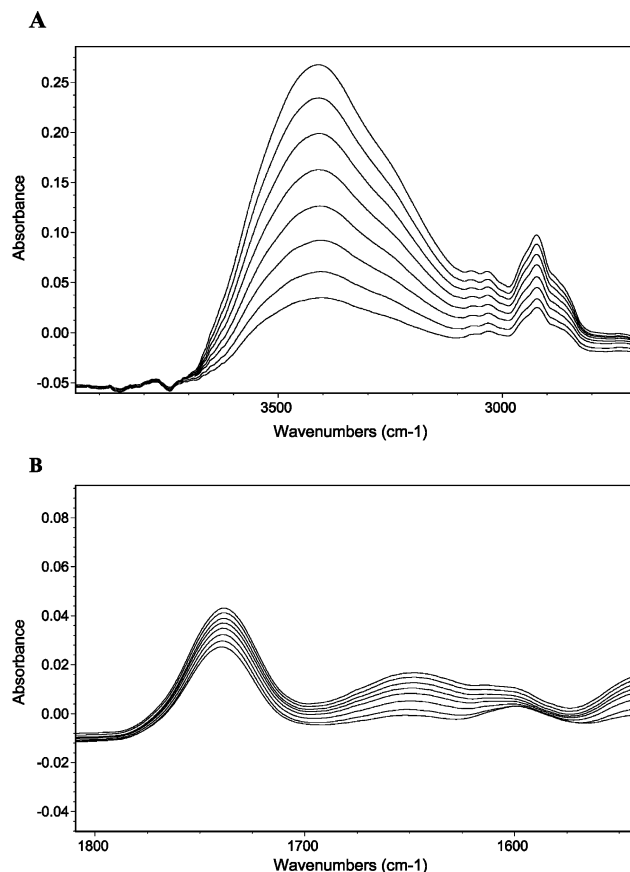


Fig. 2 Typical ATR-FTIR spectra of sorbed water in epoxy resins (in EPP) at 24 °C (A) ATR-FTIR spectra at 2700–3900 cm⁻¹ (B) ATR-FTIR spectra at 1540–1800 cm⁻¹.

Gakuin University).[†] In the 2D correlation maps unshaded regions indicate positive correlation intensities, while shaded regions indicate negative correlation intensities.

3. Results and discussion

3.1. Diffusion kinetics of glassy epoxy

It is now widely believed that the kinetics of diffusion in polymers is associated with a concentration gradient-driven diffusion process, as well as a relaxation-controlled process. Using a semi-empirical eqn. (1) expressing the initial shape of sorption curves

$$M_t/M_\infty \equiv kt^n \quad (1)$$

in which M_t and M_∞ are the mass of water sorbed at time t and at equilibrium. Three classes of diffusion behavior are distinguished, for Fickian diffusion $n = 0.5$, for Case II diffusion $n \geq 1$ and for anomalous diffusion $0.5 < n < 1$. Alfrey *et al.*²³ proposed that the rate of diffusion is much slower, much faster or more comparable than the rate of segmental relaxation respectively for these three diffusion types. The mass of sorbed water was measured by observing the variation of the absorbance intensity of OH stretching vibration band located at 3200–3800 cm⁻¹ (in Fig. 2A). The integrated area was plotted as a function of time to obtain the initial sorption curves (in Fig. 3) and the parameter n was calculated from fitting to eqn. (1). As shown in Table 1 quite consistent with the gravimetric results that among four epoxy samples the diffusion behavior of EPA and EPP were much approximate to Fickian

[†] Department of Chemistry, School of Science & Technology, Kwansei-Gakuin University 2-1 Gakuen, Sanda 669-1337 Japan

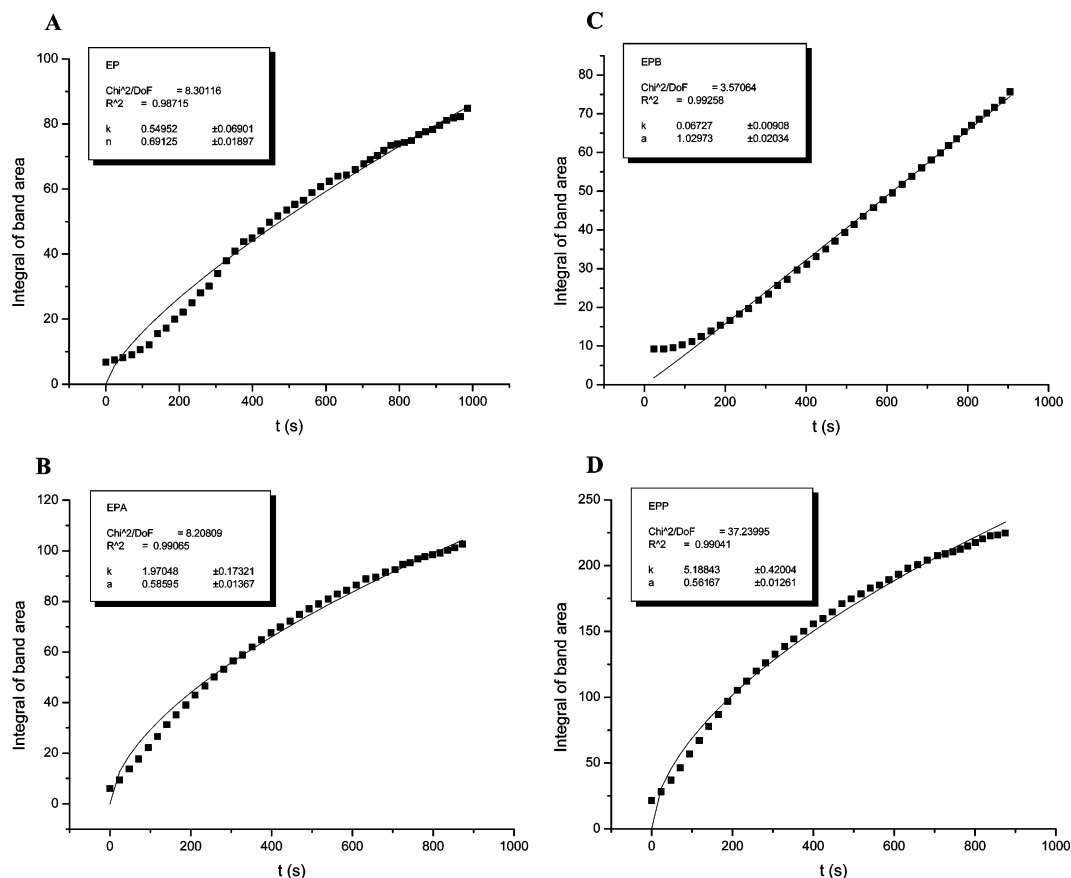


Fig. 3 Initial sorption curves fitting to equation $M_t/M_\infty = kt^n$ by ATR-FTIR measurements of epoxy resins (A) EP (B) EPA (C) EPB (D) EPP.

diffusion which means a diffusion controlled process where the diffusion rate is much slower than the polymer relaxation rate, while EPB displays a typical Case II characteristic and EP follows anomalous diffusion. Fickian diffusion often occurs in rubbery polymers possessing sufficient segment mobility to allow solvent penetration. It also commonly occurs when the activity of solvent is sufficient low or the diffusion occurs only in the free volume of the polymer. Diffusion of small molecules in glassy polymers often displays various deviations from Fickian diffusion and several different models have been proposed to describe the non-Fickian behavior. Some examples are the stress-dependent, the history-dependent and dual-phase diffusion models.^{24–27} In EP networks, the strong hydrogen bonding formed by hydroxyl groups makes the less mobility of the whole network which cumpers the segment relaxation process, as the result, epoxy segment relaxation rate is decreased to be comparable with water diffusion rate. Furthermore considering the strong hydrogen bonding interaction between water and hydrophilic groups in EP epoxy, the widely used Fickian law is less appearing since its assumption does not involve this interaction, which maybe the main reason of observed anomalous diffusion behavior. More interesting that EPB has the

lowest T_g and largest chain mobility among four epoxy samples,²² however, its diffusion behavior displays a typical Case II feature. This might be explained by the “shielding effect” of side group. The end group $CH_3CH_2CH_2-$ is hydrophobic and pliable so the accessible free volume and hydrophilic sites of water diffusion is sheltered and reduced by its rapid movement. This “shielding effect” causes the segment relaxation controlling the diffusion process.

Diffusion coefficient was calculated from ATR-FTIR spectra by a non-linear curve fit assuming Fickian diffusion, eqn. (2),¹²

$$\frac{A_t}{A_\infty} = 1 - \frac{8\gamma}{\pi[1 - \exp(2L\gamma)]} \times \sum_{n=0}^{\infty} \frac{\left[\exp\left(\frac{-D(2n+1)^2\pi^2 t}{4L^2}\right) \times \left[\frac{(2n+1)\pi}{2L} \exp(-\gamma 2L) + (-1)^n(2\gamma) \right] \right]}{(2n+1) \left(4\gamma^2 + \left(\frac{(2n+1)\pi^2}{2L} \right) \right)} \quad (2)$$

in this expression, A_t and A_∞ is the band absorbance of ATR-FTIR spectra at time t and at equilibrium respectively, L is the film thickness, the parameter γ can be defined from eqn. (3).²⁸

$$\gamma = 2n_2\pi[\sin^2\theta - (n_1/n_2)^2]^{1/2}/\lambda \quad (3)$$

where λ is the wavelength of infrared beam in the ATR element, θ is the incidence angle of radiation at the polymer/element interface, n_1 is the refractive index of IRE element and n_2 is the polymer refractive index. As shown in Table 1, the calculated diffusion coefficients of EPA and EPP from ATR-FTIR spectra are consistent with gravimetric results and the data fits very well to the Fickian eqn. (2) with little

Table 1 Calculated parameter n and diffusion coefficient D ($10^{-9} \text{ cm}^2 \text{ s}^{-1}$), Diffusion experiment was carried out at 20°C for gravimetric measurements and at 24°C for ATR-FTIR method

		EP	EPA	EPB	EPP
Gravimetric	D	2.4	9.5	—	8.4
	n	0.691	0.591	1.144	0.610
ATR-FTIR	D Value	0.4	1.9	—	1.3
	Deviation	± 0.34	± 0.14	—	± 0.06
	n Value	0.732	0.586	1.030	0.562
	Deviation	± 0.0190	± 0.0137	± 0.0203	± 0.0126

deviation, while the diffusion coefficient of EPB cannot be calculated by using Fickian diffusion equation due to it being characteristic of Case II diffusion. The data of EP display a higher deviation from the Fickian equation compared with that of EPA and EPP, additionally, the diffusion coefficient of EP is much lower than that of EPA and EPP. The reason for that is to retard the diffusion of water throughout the whole network owing to the stronger hydrogen bonding between water molecules and the epoxy networks.

3.1. Epoxy–water interaction by 2D-IR spectroscopy

The synchronous correlation spectra of EPP in the range of 2800–3700 cm^{-1} are shown in Fig. 4A. In the 1D reference spectra at the top and side of the 2D correlation maps two main bands in the range of 3200–3600 cm^{-1} and 2900–3000 cm^{-1} are assigned to the water OH stretching vibration and bulk CH vibration respectively.

An asynchronous cross peak develops only if the intensities of two dynamic bands vary out of phase, delayed or accelerated, with respect to each other.¹⁷ In the corresponding asynchronous correlation spectra (Fig. 4B) water vibration band at 3200–3600 cm^{-1} which overlapped in 1D-IR spectra is split into two separate bands ν_1 ν_2 located around 3396 and 3129 cm^{-1} in EP, 3480 and 3249 cm^{-1} in EPA, 3448 and 3263 cm^{-1} in EPB, 3457 and 3272 cm^{-1} in EPP (in Table 2). It suggests that there are two different states of water in epoxy networks. The water bands at higher wavenumber could be water molecules distributed into free volume (microvoids) or molecularly dispersed with less hydrogen bonding (bulk dissolve), while the other at lower wavenumber revealing stronger hydro-

Table 2 Band position/ cm^{-1} of two different states (bound/bulk) of water in 2D-IR spectra

		EP	EPA	EPB	EPP
2800–3700 cm^{-1}	ν_1	3396	3480	3448	3457
	ν_2	3129	3249	3263	3272
1550–1830 cm^{-1}	ν_1	1666	1654	1648	1645
	ν_2	1600	1604	1598	1598

gen bonding interaction between hydrophilic groups of epoxy networks and water molecules is attributed to bound water.

The OH band appearing from bound water in EP at 3129 cm^{-1} has a much lower wavenumber than that in EPA at 3249 cm^{-1} , EPB at 3263 cm^{-1} and EPP at 3272 cm^{-1} indicating the strength order of hydrogen bonding between water molecules and epoxy networks as EP > EPA > EPB > EPP. This epoxy–water interaction is associated tightly with side group nature of epoxy networks. The hydrogen bonding between water molecules and carboxyl groups in EPA, EPB and EPP are not as strong as that between water molecules and hydroxyl groups in EP. Furthermore, large size and hydrophobic groups Ph-CH₂ and CH₃CH₂CH₂ near carboxyl groups in EPP and EPB hinder water molecules binding with carboxyl groups in a great degree.

The sign of the asynchronous correlation peak $\psi(\nu_1, \nu_2)$ gives information about the sequential order of intensity changes between band ν_1 and band ν_2 . According to the publications of Noda¹⁷ if $\Phi(\nu_1, \nu_2) > 0$, $\psi(\nu_1, \nu_2)$ is positive (unshaded area), band ν_1 varies prior to band ν_2 , and if $\psi(\nu_1, \nu_2)$ is negative (shaded area), band ν_1 varies behind band ν_2 . In the Fig. 4B $\Psi(3457, 3272)$ is negative suggests that the band at 3272 cm^{-1} varies prior to the band at 3457 cm^{-1} . It means in EPP networks the bound water forming stronger hydrogen-bonding with epoxy networks is produced prior to the water diffused into free volume (microvoids) or water molecularly dispersed with less hydrogen bonding (bulk dissolution). The same results of EP, EPA and EPP are obtained. It is concluded that in the process of water diffusion into epoxy networks, water molecules first bind with specific hydrophilic groups as bound water and then diffuse into free volume (microvoids) or molecularly dispersed with less hydrogen bonding (bulk dissolve). In fact, at lower water concentrations strong interactions are more likely to develop for enthalpy reasons, while as the water concentration increases strongly interacting sites get closer to saturation and weak interactions play an increasingly significant role.

The synchronous correlation spectra of EPP in the range of 1500–1800 cm^{-1} are shown in Fig. 5A. In the 1D reference spectra at the top and side of the 2D correlation maps two main bands appeared in the range of 1700–1780 cm^{-1} and 1550–1680 cm^{-1} are respectively assigned to bulk CO vibration and water OH bending vibration. Epoxy networks adjust their segments to adapt water diffusion, causing relaxation of the material, therefore, the carboxyl band variation near 1750 cm^{-1} of EPA, EPB and EPP could be attributed to interaction between water molecules and epoxy carboxyl group.

The corresponding asynchronous correlation spectra in the range of 1500–1800 cm^{-1} (in Fig. 5B.) show that the splitting of water bending vibration band around 1600–1650 cm^{-1} also suggests the existence of two different states of water: distributed in free volume (microvoids) or molecularly dispersed with less hydrogen bonding (bulk dissolve) and forming stronger water–epoxy hydrogen bonding interactions as bound water. The former located at lower wave number, the latter located at higher wave number because the water bending vibration band will shift to higher wave number compared with that of free water if the water molecules formed hydrogen bonding. Similarly, the OH band of EP appearing from bound water has obviously higher wavenumber than that of EPA, EPB

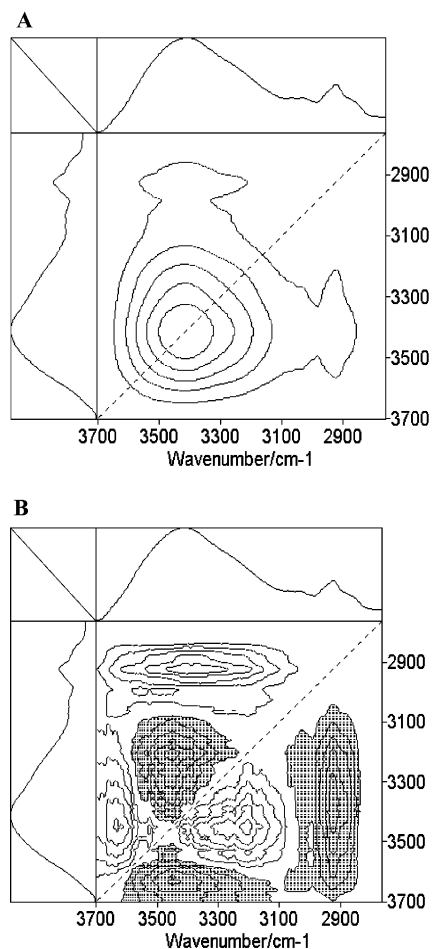


Fig. 4 Synchronous (A) and asynchronous (B) 2D correlation spectra of EPP at 2800–3700 cm^{-1} of EPP.

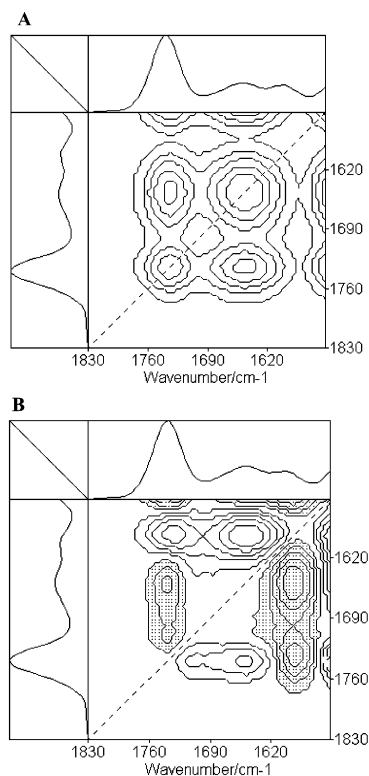


Fig. 5 Synchronous (A) and asynchronous (B) 2D correlation spectra of EPP at 1500–1800 cm^{-1} of EPP.

and EPP (in Table 2) showing the same strength order of hydrogen bond between water molecules and epoxy networks as $\text{EP} > \text{EPA} > \text{EPB} > \text{EPP}$.

Additionally, the sign of asynchronous correlation peak $\psi(\nu_1, \nu_2)$ gives information about the sequential order of two water states was quite consistent with the results of the range of 2800–3700 cm^{-1} as discussed above.

Vibrational spectroscopy has been used extensively to investigate the structure and dynamics of water in polymer system. However, in most of the previous works attention has been focused on the fundamental OH stretching vibrations of water around 3100–3700 cm^{-1} since it is the most sensitive region to the states of water and hydrogen bonding interactions. To date few studies have analyzed the OH bending modes at 1600–1700 cm^{-1} because it always overlaps with other polymer bands and cannot be effectively differentiated. In the present system no other bands coupled with the OH bending vibrations and the results of this region are very identical with the OH stretching modes.

4. Conclusion

1. The sorption curves from gravimetric and ATR-FTIR measurements of four epoxy samples show that the diffusion behavior of EPA and EPP were quite approximate to Fickian diffusion, while EPB displays a typical Case II characteristic and EP follows anomalous diffusion. The diffusion coefficients of EP, EPA and EPP were calculated from ATR-FTIR spectra, which were consistent with gravimetric results.

2. The splitting of water vibration band in two ranges of 2D-IR spectra elucidates that there exist two states of water in

epoxy networks. In the diffusion process water molecules first bind with specific hydrophilic groups as bound water and then diffuse into free volume (microvoids) or bulk dissolve as free water.

3. The wavenumber of OH band appearing from the bound water among EP, EPA, EPB and EPP indicates that the strength order of hydrogen-bonding between water molecules and epoxy networks follows as $\text{EP} > \text{EPA} > \text{EPB} > \text{EPP}$.

Acknowledgements

The author Peiyi Wu gratefully acknowledges the financial support by the National Science Foundation of China (NSFC) (No. 20274010, No. 50103003), the “Qimingxing” Project (No. 01QE14001) of Shanghai Municipal Science and Technology Commission, and the “Shuguang” Project (No. 01SG05) of the Shanghai Municipal Education Commission and Shanghai Education Development Foundation.

References

- 1 M. T. Aronhime and J. K. Gillham, *J. Appl. Polym. Sci.*, 1986, **32**, 3589.
- 2 D. Maxwell and R. A. Pethrick, *J. Appl. Polym. Sci.*, 1983, **28**, 2363.
- 3 J. M. Zhou and J. P. Lucas, *Polymer*, 1999, **40**, 5505.
- 4 L. Núñez, M. Villanueva, F. Fraga and M. R. Núñez, *J. Appl. Polym. Sci.*, 1999, **74**, 353.
- 5 G. Z. Xiao and M. E. R. Shanahan, *J. Polym. Sci. Part B: Polym. Phys.*, 1997, **35**, 2659.
- 6 C. L. Soles and A. F. Yee, *J. Polym. Sci. Part B: Polym. Phys.*, 2000, **38**, 792.
- 7 M. Woo and M. Piggott, *J. Compos. Technol. Res.*, 1987, **9**, 101.
- 8 A. Apicella, L. Nicolais and C. Decataldis, *J. Membr. Sci.*, 1985, **18**, 211.
- 9 M. Adamson, *J. Mater. Sci.*, 1980, **15**, 1736.
- 10 P. Moy and F. E. Karasz, *Polym. Eng. Sci.*, 1980, **20**, 315.
- 11 R. A. Pethrick, E. A. Hollins, I. McEwan, E. A. Pollock and D. Hayward, *Polym. Int.*, 1996, **39**, 275.
- 12 G. T. Fieldson and T. A. Barbari, *Polymer*, 1993, **34**(6), 1193.
- 13 R. Macia and Y. Jack, *J. Chem. Soc., Faraday Trans.*, 1996, **92**(15), 2731.
- 14 S. U. Hong and T. A. Barbari, *J. Polym. Sci. Part B: Polym. Phys.*, 1998, **36**, 337.
- 15 S. Cotugno and D. Larobina, *Polymer*, 2001, **42**, 6431.
- 16 C. Sammon, J. Yarwood and N. Everall, *Polymer*, 2000, **41**, 2521.
- 17 I. Noda, *Appl. Spectrosc.*, 1993, **47**, 1329.
- 18 I. Noda, *J. Am. Chem. Soc.*, 1989, **111**, 8116.
- 19 I. Noda, *Appl. Spectrosc.*, 1990, **44**, 550.
- 20 M. A. Czarnecki, P. Wu and W. H. Siesler, *Chem. Phys. Lett.*, 1998, **283**, 326.
- 21 X W. Luo, S. J. Li and W. F. Zhou, *Macromol. Rapid. Commun.*, 1995, **16**, 941.
- 22 Y. F. Ding, M. J. Liu, S. J. Li, S. Y. Zhang and W. F. Zhou, *Macromol. Chem. Phys.*, 2001, **202**, 2681.
- 23 T. Alfrey, E. F. Gurnee and W. G. Lloyd, *J. Polym. Sci., Part C: Polym. Symp.*, 1966, **12**, 2491.
- 24 J. Crank, *The Mathematics of Diffusion*, Clarendon Press, Oxford, 2nd edn., 1975.
- 25 J. Crank, G. S. Park, *Diffusion in Polymer*, Academic Press, New York, 1968.
- 26 D. R. Paul and W. J. Koros, *J. Polymer Sci, Part B: Polym. Phys.*, 1976, **146**, 675.
- 27 M. E. Gurtin and C. Yatomi, *J. Compos. Mater.*, 1979, **13**, 126.
- 28 N. J. Harric, *International Reflection Spectroscopy*, John Wiley, New York, 1967.